

# Probabilistic Forecasting via Autoregressive Flow Matching

Ahmed El-Gazzar, Marcel van Gerven

*Department of Machine Learning and Neural Computing, Donders Institute for Brain, Cognition and Behaviour, Thomas Van Aquinostraat 4, Nijmegen, 6525GD, the Netherlands*

---

## Abstract

In this work, we introduce autoregressive flow matching (AFM) for probabilistic forecasting of multivariate timeseries data. Given historical measurements and optional future covariates, we formulate forecasting as sampling from a learned conditional distribution over future trajectories. Specifically, we decompose the joint distribution of future observations into a sequence of conditional densities, each modeled via a shared flow that transforms a simple base distribution into the next observation distribution, conditioned on observed covariates. To achieve this, we leverage the flow matching framework, enabling scalable and simulation-free learning of these transformations. By combining this factorization with the flow matching objective, AFM retains the benefits of classical autoregressive models – including strong extrapolation performance, compact model size, and well-calibrated uncertainty estimates – while also capturing complex multi-modal conditional distributions, as seen in modern transport-based generative models. We demonstrate the effectiveness of AFM on multiple stochastic dynamical systems and real-world forecasting tasks.

The codebase is available at <https://github.com/elgazzarr/afm>

*Keywords:* forecasting, flow matching, generative model

---

## 1. Introduction

A core problem in modern machine learning is probabilistic timeseries forecasting, where the aim is to extrapolate how system dynamics evolve into the future given observational data. This problem is central to a wide range of scientific, industrial and societal disciplines [22, 5, 42].

An emerging trend is to leverage deep generative models to tackle this problem [16, 29, 6]. In this setting, forecasting is framed as sampling from a future probability density conditioned on the past. Most notably, diffusion models and score-based generative models [33, 12, 34] have recently pushed state-of-the-art performance in multiple forecasting benchmarks [30, 36, 17, 27]. Despite their impressive performance, diffusion models typically come with high computational costs during training and inference.

Flow matching (FM) [24, 1, 23] is an emerging paradigm for generative modeling that generalizes and subsumes diffusion models while offering more flexible design choices. Unlike diffusion

models, which rely on iterative stochastic denoising steps over a discretized trajectory, FM learns deterministic probability paths that transforms arbitrary base distributions into the target distribution directly through continuous normalizing flows. By optimally designing these probability paths, FM circumvents the need for handcrafted noise schedules and lengthy ancestral sampling chains inherent to diffusion, enabling more efficient training and sampling.

Recently, FM has been applied in the context of timeseries modeling and probabilistic forecasting [35, 13, 18], showing strong empirical results and improved computational efficiency compared to diffusion models. However, current approaches rely on directly learning the conditional distribution of an entire fixed-horizon future window conditioned on a fixed-horizon context window. While this leads to fast training and sampling, it also results in models that extrapolate poorly beyond the training distribution, and miscalibrated uncertainty estimates. Additionally, it introduces a more complex optimization problem, where models at-

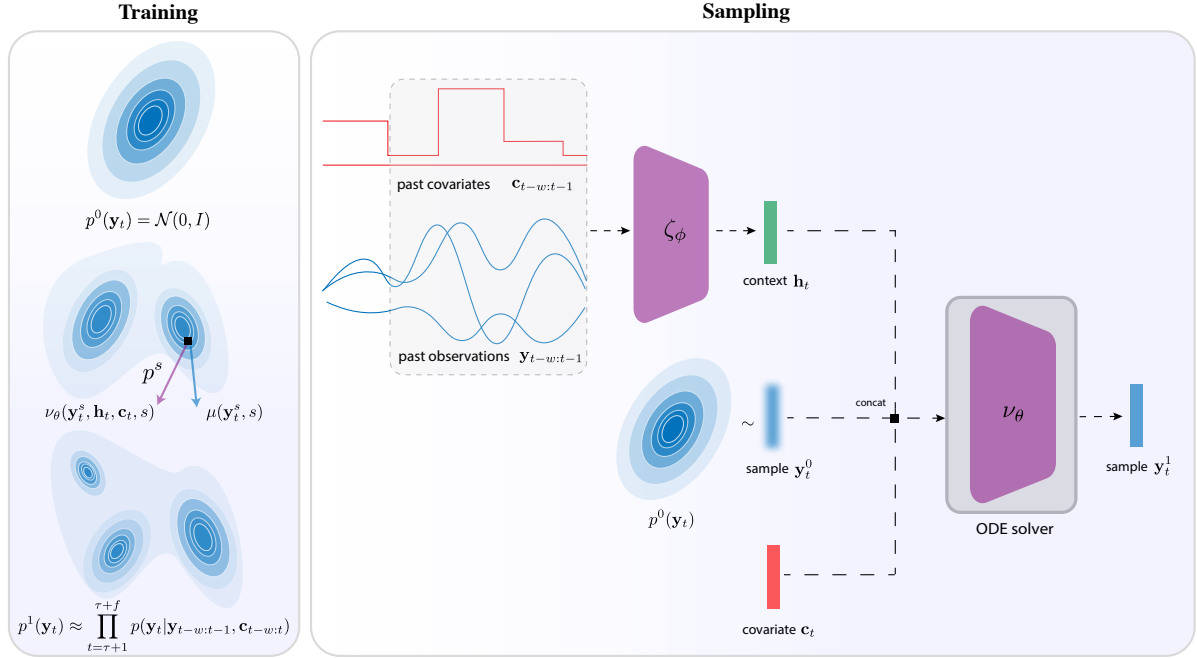


Figure 1: An overview of the training and sampling process of our approach. During training, a probability path  $(p^s)_{0 \leq s \leq 1}$  is constructed between a base distribution  $p^0$  and the target distribution  $p^1$ . This probability path is generated by a velocity field  $\mu$ . Training is done by regressing  $\mu$  via a neural network  $\nu_\theta$  which takes in a sample from the probability path  $\mathbf{y}_t^s$  at flow step  $s$ , a context vector  $\mathbf{h}_t$  encoding past observations and covariates, and the current covariate  $\mathbf{c}_t$ . After training, sampling from the target distribution is achieved via first sampling the base distribution  $p^0$ , and integrating the trained velocity field via a ODE solver until  $s = 1$ .

tempt to learn intricate time-dependent probability paths along the flow dimension. The latter issue is highlighted in [18], where the authors propose to use informed priors based on Gaussian processes to simplify and speed up optimization. However, this restricts their approach to univariate forecasting problems.

In this work, we propose autoregressive flow matching (AFM) as a simple alternative that utilizes FM to learn probabilistic forecasting models that scale to high-dimensional multivariate datasets without relying on informed priors. Unlike existing FM-based methods that model the entire future window simultaneously, AFM decomposes the forecasting problem into a sequence of conditional distributions, modeling the distribution of each future time step conditioned on past observations and covariates. This is achieved using a shared flow that transforms a simple base distribution into the next observation’s distribution. This autoregressive structure, shown in Fig. 1, enables AFM to naturally handle variable forecasting horizons, extrapolate beyond the training distribution, and provide

well-calibrated uncertainty estimates, while simplifying the optimization problem.

We demonstrate that AFM achieves superior or competitive performance on both classical dynamical systems and real-world forecasting tasks, offering a practical and effective solution to probabilistic timeseries forecasting.

## 2. Autoregressive flow matching

### 2.1. Flow matching

Standard flow matching [23] is a paradigm for generative modeling that enables training of continuous normalizing flows (CNFs) [4, 11] at an unprecedented scale. CNFs model data transformations as solutions to ordinary differential equations (ODEs), providing invertible mappings with tractable likelihoods.

Similar to CNFs, FM aims to learn a time-dependent diffeomorphic map defined on the data space  $\Omega$ , called a flow  $\psi: [0, 1] \times \Omega \rightarrow \Omega$ . This flow transforms a sample  $\mathcal{X}^0 \sim p$  from a source distribution  $p$  into a target sample  $\mathcal{X}^1 := \psi(\mathcal{X}^0, 1)$  such

that  $\mathcal{X}^1 \sim q$  for some target distribution  $q$ . The flow is constructed by solving the following initial value problem:

$$d\psi(\mathcal{X}, s) = \mu(\psi(\mathcal{X}, s), s)ds \text{ s. t. } \psi(\mathcal{X}, 0) = \mathcal{X} \quad (1)$$

where  $\mu: \Omega \times [0, 1] \rightarrow \Omega$  is a vector field defining the velocity of the flow and generating a probability path  $(p^s)_{0 \leq s \leq 1}$  where each  $p^s$  is a distribution over  $\Omega$  with  $p^0 = p$ . The objective is thus to learn a valid vector field  $\mu$  such that  $p^1 = q$ .

Unlike CNFs where the vector field is learned via likelihood maximization, requiring solving and differentiating through Eq. (1) during training, FM learns a vector field  $\nu_\theta$  with parameters  $\theta$  by regressing over vector fields of fixed conditional probability paths. This enables defining a tractable objective function called conditional flow matching (CFM) defined as:

$$\mathcal{L}_{\text{CFM}}(\theta) = \mathbb{E} \|\nu_\theta(\mathcal{X}, s) - \mu(\mathcal{X}, s | \mathcal{X}^1)\|^2 \quad (2)$$

where the expectation is taken over  $s \sim \mathcal{U}[0, 1]$ ,  $\mathcal{X}^1 \sim q(\mathcal{X}^1)$  and  $\mathcal{X} \sim p^s(\mathcal{X} | \mathcal{X}^1)$ .

Minimizing this objective allows sampling from  $q$  by solving Eq. (1) with the trained  $\nu_\theta$ . By avoiding gradient backpropagation through the ODE solver, FM enables stable and scalable training for high-dimensional generative tasks, such as image and video modeling [8, 28]. Various probability path designs and conditioning strategies have been proposed, unifying multiple transport-based generative models under this framework [24, 1, 37].

## 2.2. Autoregressive flow matching

We propose an autoregressive extension of the flow matching paradigm with the aim of improving probabilistic forecasting.

Let  $\mathbf{y}_\tau \in \mathbb{R}^n$  denote an  $n$ -dimensional observation at time  $\tau$ . Given access to its  $l$  past measurements including the current observation, denoted as  $\mathbf{Y}_l = \{\mathbf{y}_{\tau-l}, \dots, \mathbf{y}_\tau\}$ , our objective is to provide probabilistic forecasts of the next  $f$  future values denoted as  $\mathbf{Y}_f = \{\mathbf{y}_{\tau+1}, \dots, \mathbf{y}_{\tau+f}\}$ , potentially conditioned on observed covariates  $\mathbf{C} = \{\mathbf{c}_{\tau-l}, \dots, \mathbf{c}_{\tau+f}\}$  where  $\mathbf{c}_\tau \in \mathbb{R}^c$ . Formally, our goal is to learn to sample from the conditional distribution  $p(\mathbf{Y}_f | \mathbf{Y}_l, \mathbf{C})$  using a dataset  $\mathcal{D} = \{(\mathbf{Y}_f^i, \mathbf{Y}_l^i, \mathbf{C}^i)\}_{i=1}^m$  with  $m$  the number of instances.

We propose to factorize the conditional distribution autoregressively across future time-steps under

a Markov assumption of order  $w$  such that:

$$p(\mathbf{Y}_f | \mathbf{Y}_l, \mathbf{C}) = \prod_{t=\tau+1}^{\tau+f} p(\mathbf{y}_t | \mathbf{y}_{t-w:t-1}, \mathbf{c}_{t-w:t}) \quad (3)$$

where  $w \leq l$  is the history size. Our objective thus becomes learning the conditional distribution in Eq. (3). Instead of maximum likelihood estimation, as commonly used for autoregressive models, we employ the flow matching framework to learn this conditional distribution.

This autoregressive factorization provides several advantages. First, it reduces the learning problem to modeling simpler conditional distributions  $p(\mathbf{y}_t | \mathbf{y}_{t-w:t-1}, \mathbf{c}_{t-w:t})$  rather than a complex high-dimensional joint distribution. Second, each time step's conditional distribution can be trained within a teacher forcing framework allowing parallel training. Third, the Markov assumption with window size  $w$  offers a trade-off between model capacity and computational complexity. Finally, this formulation enables interpretable uncertainty quantification by explicitly modeling how prediction uncertainty propagates through time via the chain of conditional distributions.

In autoregressive flow matching, for all future time steps  $t \in [\tau + 1, \tau + f]$ , we define a target probability path  $(p^s(\mathbf{y}_t))_{0 \leq s \leq 1}$ , with marginals  $p^0(\mathbf{y}_t) = \mathcal{N}(0, I)$  and

$$p^1(\mathbf{y}_t) \approx \prod_{t=\tau+1}^{\tau+f} p(\mathbf{y}_t | \mathbf{y}_{t-w:t-1}, \mathbf{c}_{t-w:t}) \approx p_{\mathcal{D}}$$

where  $p_{\mathcal{D}}$  is the empirical distribution. This probability path is generated by a flow field  $\psi: \mathbb{R}^n \times [0, 1] \rightarrow \mathbb{R}^n$  along  $s$  defined via the ordinary differential equation (ODE):

$$d\psi(\mathbf{y}_t, s) = \mu(\psi(\mathbf{y}_t, s), s)ds \text{ s. t. } \psi(\mathbf{y}_t, 0) = \mathbf{y}_t \quad (4)$$

where  $\mu: \mathbb{R}^n \times [0, 1] \rightarrow \mathbb{R}^n$  is a vector field constructing the flow chosen such that the resulting flow satisfy the continuity equation.

To derive a tractable objective, we can model the marginal probability path as a mixture of conditional probability paths:

$$p^s(\mathbf{y}_t) = \int p^s(\mathbf{y}_t | \mathbf{z})p(\mathbf{z})d\mathbf{z} \quad (5)$$

where  $\mathbf{z} \sim \pi_{0,1}(\mathbf{z})$  is a conditioning random variable sampled from an arbitrary data coupling  $\pi_{0,1}$ .

Theorem 2 in [23] shows that the conditional velocity fields  $\mu(\mathbf{y}_t, s \mid \mathbf{z})$  associated with the conditional probability paths  $p^s(\mathbf{y}_t \mid \mathbf{z})$  are equivalent to their respective marginal velocity field  $\mu(\mathbf{y}_t, s)$ .

Following [37], we choose  $\mathbf{z} = \{\mathbf{y}_t^0, \mathbf{y}_t^1\}$  with  $p(\mathbf{z} = (\mathbf{y}_t^0, \mathbf{y}_t^1)) = p^0 \times p^1$ , where  $\mathbf{y}_t^0$  and  $\mathbf{y}_t^1$  are samples from  $p^0$  and  $p^1$ , respectively. We define the conditional probability path as:

$$p^s(\mathbf{y}_t \mid \mathbf{z}) = \mathcal{N}((1-s)\mathbf{y}_t^0 + s\mathbf{y}_t^1, \sigma^2 I) \quad (6)$$

with marginals satisfying  $p^0(\mathbf{y}_t \mid \mathbf{z}) = p^0(\mathbf{y}_t)$  and  $p^1(\mathbf{y}_t \mid \mathbf{z}) = p^1(\mathbf{y}_t)$  for  $\sigma^2 \rightarrow 0$ . The respective conditional velocity field is then simply given by  $\mu(\mathbf{y}_t, s \mid \mathbf{z}) = \mathbf{y}_t^1 - \mathbf{y}_t^0$ . This choice offers straight probability paths from the source to the target distributions in Euclidean space and closed-form solutions, enabling efficient training and sampling. Learning this velocity field allows us to sample from our target distribution  $p(\mathbf{y}_t \mid \mathbf{y}_{t-w:t-1}, \mathbf{c}_{t-w:t})$  by solving the ODE in Eq. (4) until  $s = 1$ .

### 2.3. AFM training

Similar to the standard FM setting, we learn the velocity field by regressing it against a neural network  $\nu_\theta$  with parameters  $\theta$  using the conditional flow matching objective in Eq. (2). To efficiently achieve this in our setting, we define a context vector  $\mathbf{h}_t \in \mathbb{R}^h$  that encodes the context window at time  $t$  defined as:

$$\mathbf{h}_t = \zeta_\phi(\mathbf{y}_{t-w:t-1}, \mathbf{c}_{t-w:t-1}) \quad (7)$$

where  $\zeta: \mathbb{R}^{w \times n} \times \mathbb{R}^{w \times c} \rightarrow \mathbb{R}^h$  is a neural network with parameters  $\phi$ . We can then define our learning objective as:

$$\mathcal{L}(\theta, \phi) = \mathbb{E} \|\mu(\mathbf{y}_t^s, s \mid \mathbf{z}) - \nu_\theta(\mathbf{y}_t^s, \mathbf{h}_t, \mathbf{c}_t, s)\|^2 \quad (8)$$

where the expectation is taken over  $\mathbf{z} \sim \pi_{0,1}$ ,  $s \sim \mathcal{U}(0, 1)$  and  $\mathbf{y}_t^s \sim p^s(\mathbf{y}_t \mid \mathbf{z})$ . Training proceeds by randomly sampling an observation at time point  $t$ , its associated context window and covariates from  $\mathcal{D}$ , and jointly optimising the parameters  $\phi$  and  $\theta$  by minimizing  $\mathcal{L}(\theta, \phi)$  via stochastic gradient descent. Note that this is akin to teacher forcing [40], where ground-truth past observations are fed into the model during training (rather than its own past predictions), allowing parallel training across all time-steps and avoiding error accumulation. Algorithm 1 summarizes the training procedure for autoregressive flow matching.

---

### Algorithm 1 AFM training.

---

**Require:** Dataset  $\mathcal{D} = \{(\mathbf{Y}_f^i, \mathbf{Y}_l^i, \mathbf{C}^i)\}_{i=1}^m$ , window size  $w$ , networks  $\nu_\theta, \zeta_\phi$

- 1: **while** not converged **do**
- 2:     Sample  $\mathbf{y}_t^0 \sim \mathcal{N}(0, I)$
- 3:     Sample  $(\mathbf{y}_t^1, \mathbf{y}_{t-w:t-1}, \mathbf{c}_{t-w:t}) \sim \mathcal{D}$
- 4:     Set  $\mathbf{h}_t = \zeta_\phi(\mathbf{y}_{t-w:t-1}, \mathbf{c}_{t-w:t-1})$
- 5:     Sample  $s \sim \mathcal{U}(0, 1)$
- 6:     Sample  $\mathbf{y}_t^s \sim \mathcal{N}((1-s)\mathbf{y}_t^0 + s\mathbf{y}_t^1, \sigma^2 I)$
- 7:     Set target  $\mu(\mathbf{y}_t^s, s \mid \mathbf{z}) = \mathbf{y}_t^1 - \mathbf{y}_t^0$
- 8:     Set  $\mathcal{L}_t = \|\mu(\mathbf{y}_t^s, s \mid \mathbf{z}) - \nu_\theta(\mathbf{y}_t^s, \mathbf{h}_t, \mathbf{c}_t, s)\|^2$
- 9:     Update  $\theta, \phi$  to minimize the loss
- 10: **end while**
- 11: **return**  $\nu_\theta, \zeta_\phi$

---

### 2.4. AFM inference

After training, we wish to provide probabilistic predictions for new observations  $\mathbf{Y}_l$  and corresponding covariates  $\mathbf{C}$  for  $f$  future timestamps into the future. For this we follow the sampling procedure in Algorithm 2, where predictions are made autoregressively using a rolling-window approach. This procedure can be repeated many times to obtain empirical quantiles of the uncertainty of our predictions.

---

### Algorithm 2 AFM inference.

---

**Require:** Past observations  $\mathbf{Y}_l$ , covariates  $\mathbf{C}$ , forecast horizon  $f$ , window size  $w$ , networks  $\nu_\theta, \zeta_\phi$

- 1: Initialize  $\mathbf{Y}_f \leftarrow \mathbf{Y}_l$
- 2: **for**  $t = \tau + 1$  **to**  $\tau + f$  **do**
- 3:     Set context  $\mathbf{h}_t = \zeta_\phi(\mathbf{y}_{t-w:t-1}, \mathbf{c}_{t-w:t-1})$  using the last  $w$  entries in  $\mathbf{Y}_f$
- 4:     Sample  $\mathbf{y}_t^0 \sim \mathcal{N}(0, I)$
- 5:     Set  $\psi(\mathbf{y}_t, 0) = \mathbf{y}_t^0$
- 6:     Solve  $\frac{d\psi(\mathbf{y}_t, s)}{ds} = \nu_\theta(\psi(\mathbf{y}_t, s), \mathbf{h}_t, \mathbf{c}_t, s)$  for  $s \in [0, 1]$
- 7:     Append  $\psi(\mathbf{y}_t, 1)$  to  $\mathbf{Y}_f$
- 8: **end for**
- 9: **return**  $\mathbf{Y}_f$

---

## 3. Experimental validation

In this section, we present our empirical results and compare AFM against various baselines using both data generated via simulating various dynamical systems and publicly available data for real-world use cases. AFM code is available via [https://github.com/elgazzarr/flow\\_time](https://github.com/elgazzarr/flow_time).

Table 1: Summary of stochastic dynamical systems.  $\mathbf{f}(\mathbf{x})$  denotes the drift function,  $\Theta$  the system parameters,  $\sigma$  the constant diffusion term, and  $p(\mathbf{x}(0))$  the initial condition distribution. Each system was integrated over the given interval  $[t_0, t_1]$  with 200 steps using the Euler–Heun method.

System	$f(\mathbf{x})$	$\Theta$	$\Sigma$	$p(\mathbf{x}(0))$	$[t_0, t_1]$
<b>Lorenz</b>	$f_1 = \sigma(x_2 - x_1)$	$\sigma = 10$	$(1.5, 1.5, 1.5)$	$\mathcal{U}([0, 10])$	$[0, 2]$
	$f_2 = x_1(\rho - x_3) - x_2$				
	$f_3 = x_1 x_2 - \beta x_3$				
<b>FitzHugh–Nagumo</b>	$f_1 = x_1 - \frac{x_1^3}{3} - x_2 + I$ $f_2 = \frac{x_1 + a - b x_2}{\tau}$	$a = 0.7$ $b = 0.8$ $\tau = 12.5$ $I = 0.5$	$(1.5, 1.5)$	$\mathcal{U}([-2, 2])$	$[0, 10]$
<b>Lotka–Volterra</b>	$f_1 = \alpha x_1 - \beta x_1 x_2$	$\alpha = 1.3$ $\beta = 0.9$ $\gamma = 0.8$ $\delta = 1.8$	$(1.5, 1.5)$	$\mathcal{U}([0, 5])$	$[0, 20]$
	$f_2 = -\delta x_2 + \gamma x_1 x_2$				
<b>Brusselator</b>	$f_1 = A + x_1^2 x_2 - (B + 1) x_1$	$A = 1.0$ $B = 3.0$	$(1.5, 1.5)$	$\mathcal{U}([0, 2])$	$[0, 20]$
	$f_2 = B x_1 - x_1^2 x_2$				
<b>Van der Pol</b>	$f_1 = x_2$	$\mu = 0.1$	$(1.5, 1.5)$	$\mathcal{U}([-2, 2])$	$[0, 20]$
	$f_2 = \mu(1 - x_1^2) x_2 - x_1$				

### 3.1. Simulation experiments

*Data.* We evaluated AFM on the task of forecasting five different stochastic dynamical systems: stochastic versions of the Lorenz system [25], FitzHugh–Nagumo model [9], Lotka–Volterra system [26], Brusselator [21], and Van der Pol oscillator [39].

For each system, we generated trajectories by numerically solving the corresponding stochastic differential equations (SDEs), using randomly sampled initial conditions and Brownian motion realizations. Each system has the general form

$$d\mathbf{x}(t) = \mathbf{f}(\mathbf{x}(t), t; \Theta) dt + \sigma d\mathbf{W}(t)$$

where  $f$  is the deterministic drift,  $\Theta$  are the system parameters,  $\sigma$  is a constant diffusion term, and  $\mathbf{W}(t)$  is standard Brownian motion. We sampled 2400 random initial conditions from a uniform distribution over the specified range (see Table 1) for each system and generated a trajectory for each initial condition by solving the SDE using the Euler–Heun method with fixed step size. We sampled 200 equally spaced time points for each trajectory. Out of the 200 time points in each trajectory, the first 75 were used as observed data, the next 75 for prediction, and the final 50 for extrapolation. Out of

the 2400 trajectories generated, we used 2000 for training and 400 for testing.

*Implementation details.* For these experiments we set  $\zeta_\phi$  as a two-layer bi-directional LSTM with 64 hidden units, and set  $\nu_\theta$  as a multi-layer perceptron with three hidden layers of size 64. We use Fourier positional embeddings to encode the flow step  $s$  into a 16-dimensional vector using a fixed set of frequencies and set the context length  $w$  to be equal to the prediction length. We trained our models via stochastic gradient descent using an Adam optimizer with a learning rate of 0.003 and a batch size of 128. Training until convergence took  $\sim 7$  minutes on a single A100-SXM4-40GB NVIDIA GPU.

*Baselines.* To evaluate the effectiveness of the autoregressive factorization in AFM, we compared our approach against a non-autoregressive flow-matching baseline, which directly models the joint distribution of future observations conditioned on past observations and covariates, that is,  $p^1 = p(\mathbf{Y}_f \mid \mathbf{Y}_l, \mathbf{C})$ . This approach serves as a direct ablation, isolating the effect of autoregressive factorization introduced in AFM. Note that this non-autoregressive formulation closely resembles the method proposed in [18]. Further details on this baseline are provided in Appendix A.

Table 2: Performance comparison of autoregressive (AFM) vs non-autoregressive (FM) factorization in our method for five different stochastic dynamical systems. Performance is compared in terms of average CRPS and NRMSE for both prediction and extrapolation regimens on the test set. Reported results are the mean and standard deviation across five different random seeds. Best results shown in blue.

System	Factorization	Prediction		Extrapolation	
		$\overline{\text{CRPS}} \downarrow$	NRMSE $\downarrow$	$\overline{\text{CRPS}} \downarrow$	NRMSE $\downarrow$
Lorenz	FM	$0.147 \pm 0.012$	$0.242 \pm 0.018$	$0.120 \pm 0.009$	$0.301 \pm 0.024$
	AFM	$0.090 \pm 0.008$	$0.017 \pm 0.003$	$0.137 \pm 0.011$	$0.048 \pm 0.006$
FitzHugh-Nagumo	FM	$0.165 \pm 0.014$	$0.131 \pm 0.011$	$0.214 \pm 0.016$	$0.306 \pm 0.022$
	AFM	$0.144 \pm 0.013$	$0.090 \pm 0.007$	$0.146 \pm 0.012$	$0.278 \pm 0.019$
Lotka-Volterra	FM	$0.130 \pm 0.011$	$0.266 \pm 0.019$	$0.136 \pm 0.012$	$0.502 \pm 0.033$
	AFM	$0.126 \pm 0.010$	$0.189 \pm 0.015$	$0.123 \pm 0.009$	$0.339 \pm 0.026$
Brusselator	FM	$0.217 \pm 0.016$	$0.658 \pm 0.042$	$0.238 \pm 0.019$	$1.046 \pm 0.057$
	AFM	$0.125 \pm 0.011$	$0.031 \pm 0.004$	$0.109 \pm 0.008$	$0.023 \pm 0.003$
Van der Pol	FM	$0.143 \pm 0.012$	$0.161 \pm 0.014$	$0.211 \pm 0.018$	$0.510 \pm 0.031$
	AFM	$0.225 \pm 0.017$	$0.051 \pm 0.005$	$0.282 \pm 0.021$	$0.101 \pm 0.009$

*Evaluation metrics.* To assess the model’s ability to extrapolate beyond its training distribution, we partitioned each trajectory into three segments: (1) an observation window, which serves as the historical input to the model; (2) a prediction window, which is available only during training to act as the target; and (3) an extrapolation window, which remains entirely unseen during training. Given an  $n$ -dimensional time series  $\mathbf{Y}_f = \{\mathbf{y}_{\tau+1}, \dots, \mathbf{y}_{\tau+f}\}$  and its predictive distribution or samples from our probabilistic model, we used the continuous rank probability score (CRPS) [41] for evaluating the performance of the model in uncertainty quantification and the normalized root mean square error (NRMSE) [15] to assess the accuracy of the predictions.

The continuous ranked probability score (CRPS) is a proper scoring rule commonly used to assess the quality of probabilistic forecasts. For a univariate random variable  $X$  with cumulative distribution function (CDF)  $F_X$  and an observed value  $x$ , the CRPS is defined as:

$$\text{CRPS}(F_X, x) = \int_{-\infty}^{+\infty} (F_X(y) - \mathbf{1}\{y \geq x\})^2 dy, \quad (9)$$

where  $\mathbf{1}\{\cdot\}$  is the indicator function. Intuitively, the CRPS evaluates how well the entire predictive distribution aligns with the observation  $x$ . Lower CRPS values indicate better-calibrated and more

accurate predictive distributions. In the context of time series forecasting, we can compute the CRPS for each time step in the forecasting horizon and average the results:

$$\overline{\text{CRPS}} = \frac{1}{f} \sum_{k=1}^f \text{CRPS}(F_{X_{\tau+k}}, y_{\tau+k}) \quad (10)$$

where  $F_{X_{\tau+k}}$  is the predicted CDF (or an empirical CDF from samples) at forecast horizon  $k$ , and  $y_{\tau+k}$  is the corresponding ground-truth observation.

The root mean square error (RMSE) is a standard metric for evaluating the accuracy of point forecasts. For a set of predictions  $\{\hat{y}_{\tau+1}, \dots, \hat{y}_{\tau+f}\}$  and corresponding ground-truth values  $\{y_{\tau+1}, \dots, y_{\tau+f}\}$ , the RMSE is:

$$\text{RMSE} = \sqrt{\frac{1}{f} \sum_{k=1}^f (\hat{y}_{\tau+k} - y_{\tau+k})^2}. \quad (11)$$

To make the RMSE scale-invariant and facilitate comparison across different datasets or time series with different magnitudes, we use the normalized RMSE (NRMSE)

$$\text{NRMSE} = \frac{\text{RMSE}}{\sigma_y} \quad (12)$$

where  $\sigma_y$  is the sample standard deviation of the observations. Alternatively, one could normalize by

the range of the data ( $\max(y) - \min(y)$ ) depending on the application. A lower NRMSE indicates more accurate predictions relative to the variability of the time series.

*Results.* Our results, summarized in Table 2, demonstrates that the autoregressive factorization employed in AFM significantly improves forecasting performance across multiple stochastic dynamical systems. For the prediction task, the AR approach outperforms the FM baseline in terms of NRMSE across all five systems, with particularly dramatic improvements observed in the Lorenz (0.017 vs 0.242) and Brusselator (0.031 vs 0.658) systems, representing reductions in error of 93% and 95%, respectively. The AR factorization also yields superior CRPS in four of the five systems, with only the Van der Pol oscillator showing better uncertainty quantification with the FM approach. More importantly, these improvements extend to the extrapolation regime, where autoregressive factorization maintains its advantage in NRMSE across all systems, demonstrating its superior ability to generalize beyond the training distribution. This is particularly evident in the Brusselator system, where AR factorization reduces the extrapolation NRMSE by 98% (0.023 vs 1.046).

Figure 2 illustrates the forecasting results for AFM compared to FM by generating future trajectories for four dynamical systems conditioned on observed data. AFM is shown to have much lower variance compared to the FM baseline, even allowing for accurate extrapolation of the dynamics beyond the prediction window it was trained on. These results confirm that modeling the temporal dependencies through autoregressive factorization enables AFM to better capture the underlying dynamics of complex stochastic systems, leading to more accurate predictions and improved uncertainty quantification, especially in challenging extrapolation scenarios.

### 3.2. Real-world datasets

*Data.* We evaluated AFM on the tasks of forecasting multiple univariate and multivariate timeseries with different frequencies (hourly and daily) from GluonTS [3]. Specifically, we used the following datasets: Electricity [20], Solar [20], Exchange [7], Traffic [7], and Wikipedia [10]. We used the versions preprocessed as in [31]. A summary of their properties is listed in Table 3.

Table 3: Properties of the datasets used in the experiments: dimension  $n$ , domain  $\Omega$ , frequency, total training timesteps  $T$ , and prediction length  $L$ .

Dataset	$n$	$\Omega$	freq.	$T$	$L$
Electricity	370	$\mathbb{R}^+$	hourly	5833	24
Exchange	8	$\mathbb{R}^+$	daily	6071	30
Solar	137	$\mathbb{R}^+$	hourly	7009	24
Traffic	963	(0, 1)	hourly	4001	24
Wikipedia	2000	$\mathbb{N}$	daily	792	30

*Implementation details.* We set  $\zeta_\phi$  as a three-layer bi-directional LSTM with 64 hidden units. We defined  $\nu_\theta$  via a residual neural network with five residual blocks implemented via 1-D convolutional layers with gated activation functions [38, 19]. The architecture is similar to the network used in [30] but with fewer residual blocks. We used Fourier positional embeddings to encode the flow step  $s$  into a 32-dimensional vector using a fixed set of frequencies. We used the same embedding technique to encode time-dependent covariates  $\mathbf{c}$ . We trained our models via stochastic gradient descent using an Adam optimizer with a learning rate of 0.001 and a batch size of 128. Depending on the dataset, training until convergence took from 40 – 100 minutes on a single A100-SXM4-40GB NVIDIA GPU.

*Baselines.* We compared AFM against multiple established baselines. These include traditional statistical methods such as Seasonal Naive (SN), AutoARIMA, and AutoETS [14], as well as deep learning methods such as DeepAR [32], WaveNet [38]. We further include diffusion baselines such as TS-Diff [17], SSSD [2], and TimeGrad [30] and a flow matching baseline TSFlow [18].

*Results.* Table 4 presents the comparison of our proposed AFM model against various baselines on five real-world timeseries datasets. The results demonstrate that AFM achieves state-of-the-art performance on three of the five datasets: Electricity, Exchange, and Solar. On the Electricity dataset, AFM outperforms all baselines with a CRPS of 0.042, representing a 6.7% improvement over the second-best model, TSFlow (0.045), and a 12.5% improvement over the autoregressive diffusion baseline TimeGrad (0.048). For the Exchange dataset, AFM matches the performance of TSFlow with a CRPS of 0.009, significantly outperforming traditional statistical methods and other deep learning approaches. Most notably, on the Solar

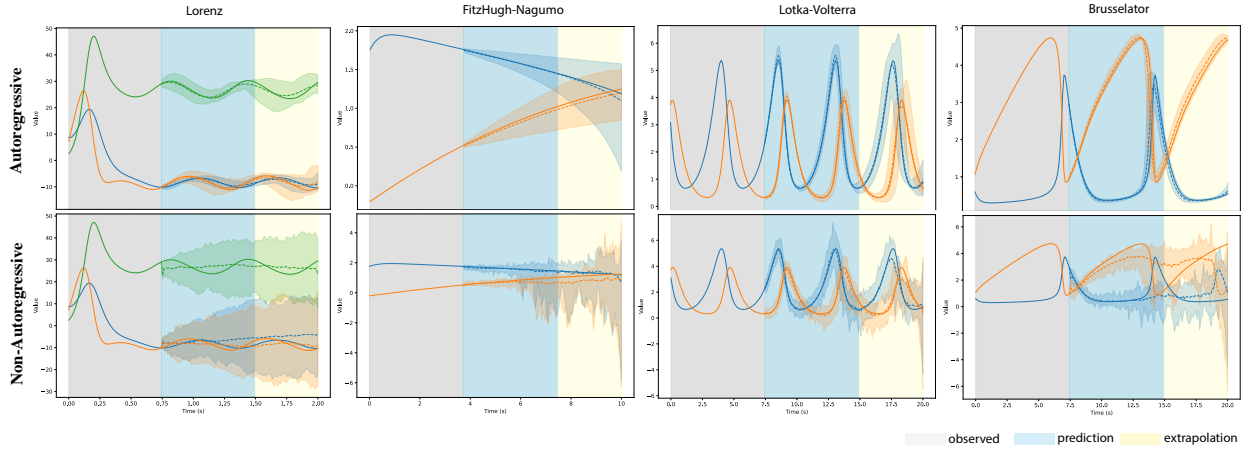


Figure 2: Samples from the forecasting results for autoregressive flow matching vs standard flow matching on four different dynamical systems. The solid lines indicate ground truth, while the dashed lines indicated the mean prediction along with the 95% confidence interval. The results are visualized during both prediction and extrapolation regimes.

Table 4: Test set average CRPS comparison (lower is better) of different models on forecasting of five real world data sets. Mean and standard error metrics for AFM obtained by re-training and evaluating five times. Results for the baselines are from [18] and [30]. Best scores in blue and second best in green.

Method	Electricity	Exchange	Solar	Traffic	Wikipedia
SN	$0.060 \pm 0.000$	$0.013 \pm 0.000$	$0.512 \pm 0.000$	$0.221 \pm 0.000$	$0.423 \pm 0.000$
ARIMA	$0.344 \pm 0.000$	$0.013 \pm 0.000$	$0.558 \pm 0.003$	$0.486 \pm 0.000$	$0.654 \pm 0.000$
ETS	$0.056 \pm 0.000$	$0.008 \pm 0.000$	$0.550 \pm 0.000$	$0.492 \pm 0.000$	$0.651 \pm 0.000$
DeepAR	$0.051 \pm 0.000$	$0.013 \pm 0.004$	$0.429 \pm 0.015$	$0.103 \pm 0.000$	$0.215 \pm 0.003$
WaveNet	$0.058 \pm 0.008$	$0.012 \pm 0.001$	$0.360 \pm 0.000$	$0.099 \pm 0.000$	$0.207 \pm 0.000$
CSDI	$0.051 \pm 0.000$	$0.013 \pm 0.000$	$0.360 \pm 0.000$	$0.152 \pm 0.000$	$0.318 \pm 0.012$
SSSD	$0.048 \pm 0.000$	$0.010 \pm 0.000$	$0.354 \pm 0.024$	$0.107 \pm 0.002$	$0.209 \pm 0.000$
TimeGrad	$0.048 \pm 0.001$	$0.013 \pm 0.002$	$0.347 \pm 0.024$	$0.109 \pm 0.002$	$0.311 \pm 0.002$
TSFlow	$0.045 \pm 0.001$	$0.009 \pm 0.001$	$0.343 \pm 0.002$	$0.083 \pm 0.000$	$0.227 \pm 0.000$
AFM	$0.042 \pm 0.001$	$0.009 \pm 0.001$	$0.284 \pm 0.002$	$0.089 \pm 0.000$	$0.243 \pm 0.002$

dataset, AFM achieves a substantial improvement with a CRPS of 0.284, representing a 17.2% reduction in error compared to TSFlow (0.343) and an 18.2% improvement over TimeGrad (0.347). While AFM ranks second on the Traffic dataset with a CRPS of 0.089, slightly behind TSFlow (0.083), it still outperforms all other traditional and deep learning baselines including TimeGrad (0.109). On the Wikipedia dataset, WaveNet (0.207) and SSSD (0.209) achieve the best performance, with TSFlow (0.227) outperforming AFM (0.243).

*Efficiency.* Table 5 presents the computational efficiency analysis. AFM achieves the best predictive performance with the smallest model size (0.85M parameters compared to 4.1M for TSFlow and 2.8M for TimeGrad). In terms of inference time, AFM

requires 180ms per forecast, which is 4x slower than the non-autoregressive TSFlow (45ms) but significantly faster than the autoregressive diffusion baseline TimeGrad (850ms). This demonstrates that AFM’s autoregressive flow matching framework with straight probability paths provides computational advantages over diffusion-based autoregressive approaches while maintaining compact model architectures. These results demonstrate that the autoregressive flow-matching approach employed in AFM consistently delivers superior or competitive performance across diverse real-world timeseries forecasting tasks, with favorable trade-offs between model size, inference speed, and predictive accuracy.

Table 5: Model efficiency comparison showing number of parameters and inference time per forecast on the Electricity and Solar datasets. AFM achieves the best accuracy with the smallest model size, while being  $4\times$  slower than the non-autoregressive TSFlow but significantly faster than the autoregressive diffusion baseline TimeGrad.

Method	Parameters	Inference Time	Electricity	Solar
TSFlow	4.1M	<b>45ms</b>	$0.045 \pm 0.001$	$0.343 \pm 0.002$
TimeGrad	2.8M	850ms	$0.048 \pm 0.001$	$0.347 \pm 0.024$
AFM	<b>0.85M</b>	180ms	<b><math>0.042 \pm 0.001</math></b>	<b><math>0.284 \pm 0.002</math></b>

## 4. Discussion

In this work, we introduced AFM, a probabilistic forecasting model that combines autoregressive modeling with flow matching to generate accurate and well-calibrated predictions for multivariate timeseries data. By factorizing the forecasting problem into a sequence of conditional distributions, AFM effectively balances the sequential dependencies in temporal data with the expressiveness of flow-based generative modeling. Our empirical results across simulated dynamical systems and real-world datasets demonstrate that AFM achieves competitive performance with state-of-the-art baselines in challenging forecasting benchmarks. The autoregressive decomposition leads to notable improvements in uncertainty calibration and distribution coverage compared to standard flow-matching approaches that model entire future windows simultaneously. Furthermore, AFM exhibits robust generalization to out-of-distribution scenarios, particularly in extrapolation tasks where it achieves 93–98% error reduction compared to non-autoregressive baselines (e.g., Brusselator: NRMSE 0.023 vs 1.046), a critical capability for real-world deployment where test conditions often diverge from training data.

AFM has limitations that warrant discussion. First, the sequential nature of autoregressive sampling introduces computational overhead during inference compared to fully parallelizable non-autoregressive models. Our experiments show that AFM is  $4\times$  slower than non-autoregressive flow matching approaches (180ms vs 45ms per forecast on real-world datasets), which may limit its applicability in real-time forecasting systems requiring latency below 50ms. However, AFM remains significantly faster than autoregressive diffusion baselines like TimeGrad (850ms) while achieving better predictive performance with smaller model sizes (0.85M vs 2.8M–4.1M parameters). Non-autoregressive methods are preferable when: (1)

real-time inference is critical with strict latency requirements ( $<50\text{ms}$ ), (2) forecast horizons are very short (1–5 steps) where the benefits of autoregressive modeling are minimal, and (3) training data fully covers the target prediction horizon and extrapolation beyond the training distribution is not required. In contrast, AFM excels in applications where accuracy and well-calibrated uncertainty estimates are prioritized over inference speed, such as climate modeling, demand planning, and scientific forecasting tasks that involve extrapolation. Additionally, our current implementation applies flow matching directly in the data space, which may be suboptimal for high-dimensional partially observed data. Future work could explore latent-space formulations, extend to irregularly sampled data, investigate adaptive window sizes that balance the trade-off between model capacity and computational efficiency, and explore broader applications in scientific modeling and decision-making under uncertainty. Overall, AFM represents a step forward in probabilistic timeseries forecasting, demonstrating the potential of flow-based generative models for improving both accuracy and uncertainty quantification while maintaining computational efficiency relative to diffusion-based approaches.

## Acknowledgements

This publication is part of the project Dutch Brain Interface Initiative (DBI2) with project number 024.005.022 of the research programme Gravitation, which was financed by the Dutch Ministry of Education, Culture and Science (OCW) via the Dutch Research Council (NWO).

## References

- [1] Michael S Albergo, Nicholas M Boffi, and Eric Vanden-Eijnden. Stochastic interpolants: A unifying framework for flows and diffusions. *arXiv preprint arXiv:2303.08797*, 2023.

[2] Juan Miguel Lopez Alcaraz and Nils Strodthoff. Diffusion-based time series imputation and forecasting with structured state space models. *arXiv preprint arXiv:2208.09399*, 2022.

[3] Alexander Alexandrov, Konstantinos Benidis, Michael Bohlke-Schneider, Valentin Flunkert, Jan Gasthaus, Tim Januschowski, Danielle C Maddix, Syama Rangapuram, David Salinas, Jasper Schulz, et al. GluonTS: Probabilistic and neural time series modeling in python. *Journal of Machine Learning Research*, 21(116):1–6, 2020.

[4] Ricky TQ Chen, Yulia Rubanova, Jesse Bettencourt, and David K Duvenaud. Neural ordinary differential equations. *Advances in Neural Information Processing Systems*, 31, 2018.

[5] Fatoumata Dama and Christine Sinoquet. Time series analysis and modeling to forecast: a survey. In *ArXiv:2104.00164*, 2021.

[6] Abhyuday Desai, Cynthia Freeman, Zuhui Wang, and Ian Beaver. TimeVAE: A variational auto-encoder for multivariate time series generation. *arXiv preprint arXiv:2111.08095*, 2021.

[7] Dheeru Dua, Casey Graff, et al. UCI machine learning repository. URL <http://archive.ics.uci.edu/ml>, 7(1):62, 2017.

[8] Patrick Esser, Sumith Kulal, Andreas Blattmann, Rahim Entezari, Jonas Müller, Harry Saini, Yam Levi, Dominik Lorenz, Axel Sauer, Frederic Boesel, et al. Scaling rectified flow transformers for high-resolution image synthesis. In *Forty-first International Conference on Machine Learning*, 2024.

[9] Richard FitzHugh. Impulses and physiological states in theoretical models of nerve membrane. *Biophysical Journal*, 1(6):445–466, 1961. doi: 10.1016/S0006-3495(61)86902-6.

[10] Jan Gasthaus, Konstantinos Benidis, Yuyang Wang, Syama Sundar Rangapuram, David Salinas, Valentin Flunkert, and Tim Januschowski. Probabilistic forecasting with spline quantile function RNNs. In *The 22nd International Conference on Artificial Intelligence and Statistics*, pp. 1901–1910. PMLR, 2019.

[11] Will Grathwohl, Ricky TQ Chen, Jesse Bettencourt, Ilya Sutskever, and David Duvenaud. FFJORD: Free-Form continuous dynamics for scalable reversible generative models. In *International Conference on Learning Representations*, 2018.

[12] Jonathan Ho, Ajay Jain, and Pieter Abbeel. Denoising diffusion probabilistic models. *Advances in Neural Information Processing Systems*, 33:6840–6851, 2020.

[13] Yang Hu, Xiao Wang, Lirong Wu, Huatian Zhang, Stan Z. Li, Sheng Wang, and Tianlong Chen. FM-TS: Flow matching for time series generation. In *ArXiv:2411.07506v1 [cs.LG]*, 2024. URL <http://arxiv.org/abs/2411.07506>.

[14] Rob Hyndman, Anne B Koehler, J Keith Ord, and Ralph D Snyder. *Forecasting with Exponential Smoothing: The State Space Approach*. Springer Science & Business Media, 2008.

[15] Rob J Hyndman and Anne B Koehler. Another look at measures of forecast accuracy. *International Journal of Forecasting*, 22(4):679–688, 2006.

[16] Maximilian Karl, Maximilian Soelch, Justin Bayer, and Patrick Van der Smagt. Deep variational Bayes filters: Unsupervised learning of state space models from raw data. *arXiv preprint arXiv:1605.06432*, 2016.

[17] Marcel Kolloviev, Abdul Fatir Ansari, Michael Bohlke-Schneider, Jasper Zschiegner, Hao Wang, and Yuyang Bernie Wang. Predict, refine, synthesize: Self-guiding diffusion models for probabilistic time series forecasting. *Advances in Neural Information Processing Systems*, 36:28341–28364, 2023.

[18] Marcel Kolloviev, Marten Lienen, David Lüdke, Leo Schwinn, and Stephan Günemann. Flow matching with gaussian process priors for probabilistic time series forecasting. In *The Thirteenth International Conference on Learning Representations*, 2024.

[19] Zhifeng Kong, Wei Ping, Jiaji Huang, Kexin Zhao, and Bryan Catanzaro. DiffWave: A versatile diffusion model for audio synthesis. *arXiv preprint arXiv:2009.09761*, 2020.

[20] Guokun Lai, Wei-Cheng Chang, Yiming Yang, and Hanxiao Liu. Modeling long- and short-term temporal patterns with deep neural networks. In *The 41st International ACM SIGIR Conference on Research & Development in Information Retrieval*, pp. 95–104, 2018.

[21] R. Lefever and I. Prigogine. Symmetry breaking instabilities in dissipative systems. II. *The Journal of Chemical Physics*, 48(4):1695–1700, 1968. doi: 10.1063/1.1668896.

[22] Bryan Lim and Stefan Zohren. Time-series forecasting with deep learning: A survey. *Philosophical Transactions of the Royal Society A*, 379(2194):20200209, 2021.

[23] Yaron Lipman, Ricky TQ Chen, Heli Ben-Hamu, Maximilian Nickel, and Matthew Le. Flow matching for generative modeling. In *The Eleventh International Conference on Learning Representations*, 2022.

[24] Xingchao Liu, Chengyue Gong, et al. Flow straight and fast: Learning to generate and transfer data with rectified flow. In *The Eleventh International Conference on Learning Representations*, 2022.

[25] Edward Lorenz. Deterministic nonperiodic flow. *Journal of Atmospheric Sciences*, 20(2), 1963.

[26] Alfred J. Lotka. *Elements of Physical Biology*. Williams & Wilkins, 1925.

[27] Caspar Meijer and Lydia Y Chen. The rise of diffusion models in time-series forecasting. *arXiv preprint arXiv:2401.03006*, 2024.

[28] Adam Polyak, Amit Zohar, Andrew Brown, Andros Tjandra, Animesh Sinha, Ann Lee, Apoorv Vyas, Bowen Shi, Chih-Yao Ma, Ching-Yao Chuang, et al. MovieGen: A cast of media foundation models. *arXiv e-prints*, pp. arXiv–2410, 2024.

[29] Kashif Rasul, Abdul-Saboor Sheikh, Ingmar Schuster, Urs Bergmann, and Roland Vollgraf. Multivariate probabilistic time series forecasting via conditioned normalizing flows. *arXiv preprint arXiv:2002.06103*, 2020.

[30] Kashif Rasul, Calvin Seward, Ingmar Schuster, and Roland Vollgraf. Autoregressive denoising diffusion models for multivariate probabilistic time series forecasting. In *International Conference on Machine Learning*, pp. 8857–8868. PMLR, 2021.

[31] David Salinas, Michael Bohlke-Schneider, Laurent Callot, Roberto Medico, and Jan Gasthaus. High-dimensional multivariate forecasting with low-rank gaussian copula processes. *Advances in Neural Information Processing Systems*, 32, 2019.

[32] David Salinas, Valentin Flunkert, Jan Gasthaus, and Tim Januschowski. DeepAR: Probabilistic forecasting with autoregressive recurrent networks. *International Journal of Forecasting*, 36(3):1181–1191, 2020.

[33] Jascha Sohl-Dickstein, Eric Weiss, Niru Maheswaranathan, and Surya Ganguli. Deep unsupervised learning using nonequilibrium thermodynamics. In *International Conference on Machine Learning*, pp. 2256–2265. PMLR, 2015.

[34] Yang Song, Jascha Sohl-Dickstein, Diederik P Kingma, Abhishek Kumar, Stefano Ermon, and Ben Poole. Score-based generative modeling through stochastic differential equations. *arXiv preprint arXiv:2011.13456*, 2020.

[35] Ella Tamir, Najwa Laabid, Markus Heinonen, Vikas Garg, and Arno Solin. Conditional flow matching for time series modelling. In *ICML Workshop: Structured Probabilistic Inference and Generative Modeling*, 2024.

[36] Yusuke Tashiro, Jiaming Song, Yang Song, and Stefano Ermon. CSDI: Conditional score-based diffusion models for probabilistic time series imputation. *Advances in Neural Information Processing Systems*, 34:24804–24816, 2021.

[37] Alexander Tong, Kilian Fatras, Nikolay Malkin, Guillaume Huguet, Yanlei Zhang, Jarid Rector-Brooks, Guy Wolf, and Yoshua Bengio. Improving and generalizing flow-based generative models with minibatch optimal transport. *arXiv preprint arXiv:2302.00482*, 2023.

[38] Aaron Van Den Oord, Sander Dieleman, Heiga Zen, Karen Simonyan, Oriol Vinyals, Alex

Graves, Nal Kalchbrenner, Andrew Senior, Koray Kavukcuoglu, et al. WaveNet: A generative model for raw audio. *arXiv preprint arXiv:1609.03499*, 12, 2016.

[39] B. van der Pol. On 'relaxation-oscillations'. *The London, Edinburgh, and Dublin Philosophical Magazine and Journal of Science*, 2(11):978–992, 1926. doi: 10.1080/14786442608564127.

[40] Ronald J Williams and David Zipser. A learning algorithm for continually running fully recurrent neural networks. *Neural Computation*, 1(2):270–280, 1989.

[41] Robert L Winkler, Javier Munoz, José L Cervera, José M Bernardo, Gail Blattenberger, Joseph B Kadane, Dennis V Lindley, Allan H Murphy, Robert M Oliver, and David Ríos-Insua. Scoring rules and the evaluation of probabilities. *Test*, 5:1–60, 1996.

[42] Jiexia Ye, Weiqi Zhang, Ke Yi, Yongzi Yu, Ziyue Li, Jia Li, and Fugee Tsung. A survey of time series foundation models: Generalizing time series representation with large language model. In *ArXiv:2104.00164*, 2024.

## Appendix A. Standard FM baseline

*Problem Setting.* We consider the same forecasting setup as in Section 2.2 where given past observations  $\mathbf{Y}_l$  and covariates  $\mathbf{C}$ , our goal remains to model the conditional distribution  $p(\mathbf{Y}_f \mid \mathbf{Y}_l, \mathbf{C})$ . However, unlike the autoregressive factorization, we directly model the joint distribution of the entire future trajectory  $\mathbf{Y}_f \in \mathbb{R}^{f \times n}$  without temporal factorization:

$$p(\mathbf{Y}_f \mid \mathbf{Y}_l, \mathbf{C}) = p(\mathbf{y}_{\tau+1}, \dots, \mathbf{y}_{\tau+f} \mid \mathbf{Y}_l, \mathbf{C}). \quad (\text{A.1})$$

This formulation preserves temporal correlations across all future time steps but requires learning a high-dimensional distribution.

*Training.* We construct a probability path  $(p^s(\mathbf{Y}_f))^{0 \leq s \leq 1}$  that transports samples from a prior distribution  $p^0(\mathbf{Y}_f) = \mathcal{N}(0, \Sigma)$  to the target distribution  $p^1(\mathbf{Y}_f) \approx p(\mathbf{Y}_f \mid \mathbf{Y}_l, \mathbf{C})$ , where  $\Sigma$  is a block-diagonal covariance matrix. The prior can be interpreted as independent Brownian motion processes per dimension, where Brownian motion is defined as a stochastic process  $W: [\tau + 1, \tau + f] \rightarrow \mathbb{R}^n$ .

We define the conditional probability path using a linear interpolation bridge with Brownian noise:

$$p^s(\mathbf{Y}_f \mid \mathbf{z}) = \mathcal{N}(\mathbf{m}_s, \sigma^2 s(1-s)\Sigma) \quad (\text{A.2})$$

where  $\mathbf{m}_s = (1-s)\mathbf{Y}_f^0 + s\mathbf{Y}_f^1$  and  $\mathbf{z} = (\mathbf{Y}_f^0, \mathbf{Y}_f^1)$  with  $\mathbf{Y}_f^0 \sim p^0$  and  $\mathbf{Y}_f^1 \sim p^1$ . The corresponding conditional velocity field becomes:

$$\mu(\mathbf{Y}_f, s \mid \mathbf{z}) = \mathbf{Y}_f^1 - \mathbf{Y}_f^0 + \frac{\sigma^2(1-2s)}{2}\Sigma^{-1}(\mathbf{Y}_f - \mathbf{m}_s) \quad (\text{A.3})$$

When  $\sigma^2 \rightarrow 0$ , this reduces to the straight path velocity  $\mu(\mathbf{Y}_f, s \mid \mathbf{z}) = \mathbf{Y}_f^1 - \mathbf{Y}_f^0$ . We learn a neural velocity field  $\nu_\theta$  that operates on the entire future trajectory. The context encoding remains similar to Eq. (7):

$$\mathbf{h} = \zeta_\phi(\mathbf{Y}_l, \mathbf{C}_{\tau-l:\tau+f}) \quad (\text{A.4})$$

where  $\zeta_\phi$  now processes both past and future covariates. The training objective becomes:

$$\mathcal{L}(\theta, \phi) = \mathbb{E} \|\mu(\mathbf{Y}_f^s, s \mid \mathbf{z}) - \nu_\theta(\mathbf{Y}_f^s, \mathbf{h}, \mathbf{C}_{\tau+1:\tau+f}, s)\|^2 \quad (\text{A.5})$$

where the expectation is taken over  $\mathbf{z} \sim \pi_{0,1}$ ,  $s \sim \mathcal{U}(0, 1)$  and  $\mathbf{Y}_f^s \sim p^s(\mathbf{Y}_f \mid \mathbf{z})$ . The vector field  $\nu_\theta$  is implemented as a sequential neural network (e.g.,

---

### Algorithm 3 FM training.

---

**Require:** Dataset  $\mathcal{D}$ , networks  $\nu_\theta, \zeta_\phi$

- 1: **while** not converged **do**
- 2:    Sample  $\mathbf{Y}_f^0 \sim \mathcal{N}(0, \Sigma)$
- 3:    Sample  $(\mathbf{Y}_f^1, \mathbf{Y}_l, \mathbf{C}) \sim \mathcal{D}$
- 4:    Set  $\mathbf{h} = \zeta_\phi(\mathbf{Y}_l, \mathbf{C}_{\tau-l:\tau+f})$
- 5:    Sample  $s \sim \mathcal{U}(0, 1)$
- 6:    Sample  $\mathbf{Y}_f^s \sim \mathcal{N}(\mathbf{m}_s, \sigma^2 s(1-s)\Sigma)$  with  $\mathbf{m}_s = (1-s)\mathbf{Y}_f^0 + s\mathbf{Y}_f^1$
- 7:    Set target  $\mu(\mathbf{Y}_f^s, s \mid \mathbf{z})$
- 8:    Set  $\mathcal{L} = \|\mu(\cdot) - \nu_\theta(\mathbf{Y}_f^s, \mathbf{h}, \mathbf{C}_{\tau+1:\tau+f}, s)\|_{\Sigma^{-1}}^2$
- 9:    Update  $\theta, \phi$  to minimize the loss
- 10: **end while**

---



---

### Algorithm 4 FM inference.

---

**Require:**  $\mathbf{Y}_l, \mathbf{C}$ , networks  $\nu_\theta, \zeta_\phi$

- 1: Encode context  $\mathbf{h} = \zeta_\phi(\mathbf{Y}_l, \mathbf{C})$
- 2: Sample initial trajectory  $\mathbf{Y}_f^0 \sim \mathcal{N}(0, \Sigma)$
- 3: Solve  $\frac{d\psi(\mathbf{Y}_f, s)}{ds} = \nu_\theta(\psi(\mathbf{Y}_f, s), \mathbf{h}, \mathbf{C}_{\tau+1:\tau+f}, s)$
- 4: Return  $\psi(\mathbf{Y}_f, 1)$

---

Transformer or RNN) that processes the entire trajectory. Sampling requires solving the trajectory-level ODE:

$$\frac{d\psi(\mathbf{Y}_f, s)}{ds} = \nu_\theta(\psi(\mathbf{Y}_f, s), \mathbf{h}, \mathbf{C}_{\tau+1:\tau+f}, s) \quad (\text{A.6})$$

using numerical solvers subject to  $\psi(\mathbf{Y}_f, 0) \sim p^0$ . This produces joint samples from  $p(\mathbf{Y}_f \mid \mathbf{Y}_l, \mathbf{C})$  without autoregressive decomposition.

Algorithms 3 and 4 describe training and inference procedures for the standard FM model, respectively.

*Implementation Details.* We used this baseline to conduct experiments on the task of forecasting multiple dynamical systems. For this setup we set  $\nu_\theta$  as a 4-layer bi-directional LSTM with 128 hidden units. We kept the same training parameters as in Section 3.1. Training until convergence took  $\sim 2$  minutes on a single A100-SXM4-40GB NVIDIA GPU.

*Key Differences from Autoregressive Variant.* The non-autoregressive approach differs fundamentally from its autoregressive counterpart introduced in AFM. First, while the autoregressive method factorizes the joint distribution via a Markovian decomposition across time steps, the non-autoregressive baseline directly models the full future trajectory  $\mathbf{Y}_f$  as a single high-dimensional ran-

dom variable. This preserves cross-temporal dependencies at the expense of learning a more complex distribution over  $\mathbb{R}^{n \times f}$ . Second, computational characteristics diverge significantly: the non-autoregressive version processes entire trajectories through sequential neural networks for the velocity fields enabling parallel generation of all future timepoints at the cost of higher memory requirements. Finally, their uncertainty propagation mechanisms contrast sharply: the autoregressive approach explicitly models how prediction errors accumulate through the chain of conditional distributions, while the non-autoregressive method captures joint uncertainty over all timesteps through trajectory-level sampling but lacks explicit mechanisms to model error accumulation dynamics. These differences create complementary trade-offs as the autoregressive variant offers interpretable uncertainty quantification and efficient window-based computation but assumes limited Markovian dependencies. In contrast, the non-autoregressive baseline preserves full temporal correlations at higher computational cost with less explicit uncertainty dynamics.